# Organic & Biomolecular Chemistry

Accepted Manuscript






ROYAL SOCIETY OF CHEMISTRY

www.rsc.org/obc

# Performance of DFT Methods and Origin of Stereoselectivity in Bipyridine *N,N′*-Dioxide Catalyzed Allylation and Propargylation Reactions

Diana Sepúlveda, Tongxiang Lu, and Steven E. Wheeler*

*Department of Chemistry, Texas A&M University, College Station, TX 77843*

Email: wheeler@chem.tamu.edu

**ABSTRACT**

Enantioselectivities for the allylation and propargylation of benzaldehyde catalyzed by bipyridine *N,N′*-dioxides were predicted using popular DFT methods. The results reveal deficiencies of several DFT methods while also providing a new explanation for the stereoselectivity of these reactions. In particular, even though many DFT methods provide accurate predictions of experimental *ee*'s for these reactions, these predictions sometimes stem from qualitatively incorrect transition states. Overall, B97-D/TZV(2*d*,2*p*) provides the best compromise between accurate predictions of low-lying transition states and stereoselectivities for these reactions. The origin of stereoselectivity in these reactions was also examined, and arises from electrostatic interactions within the chiral electrostatic environment of a hexacoordinate silicon intermediate; the previously published transition state model for these reactions is flawed. Ultimately, these results suggest two strategies for the design of highly stereoselective catalysts for the propargylation of aromatic aldehydes, and pave the way for the computational design of novel catalysts for these reactions.

## I. Introduction

Density functional theory (DFT) has emerged as a powerful tool for understanding the origin of stereoselectivity in organocatalytic reactions, and, ultimately, for the rational design of new organocatalysts.[1-7] However, this requires DFT methods that can faithfully predict the stereocontrolling transition state (TS) structures for such reactions. In order to assess the performance of popular DFT methods, we studied the bipyridine *N*,*N*′-dioxide of Nakajima and coworkers,[8-10] since it is one of the few known organocatalysts to work for both asymmetric allylation and propargylation reactions. Catalyst (*S*)-**1** reacts under similar conditions with either allyl or allenyl tricholorosilanes to afford enantioenriched alcohols (see Figure 1). However, the stereoselectivity for propargylation reactions (52% *ee*) is noticeably less than that observed for allylations (88% *ee*), despite the outward similarity of these two reactions. Our goal in this work is two-fold: First, to assess the performance of DFT methods applied to these reactions in order to identify approaches that provide reliable predictions of relative barrier heights as well as stereoselectivities of these reactions, and second, to explain the origin of stereoselectivity of allylations catalyzed by (*S*)-**1** as well as the reduced stereoselectivity in the case of propargylation reactions. This builds on our previous work[11-12] on bipyridine *N*-oxide catalysts for asymmetric alkylation reactions, and will also lay the groundwork for the computational design of bipyridine *N*,*N*′-dioxide catalysts for asymmetric propargylations.

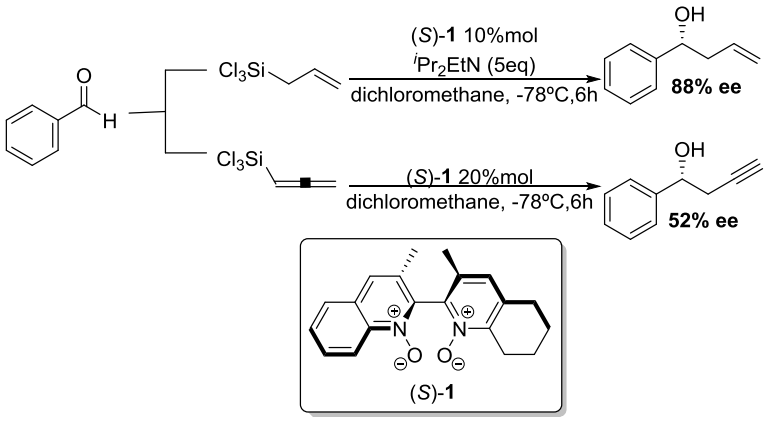


**Figure 1.** Allylation and propargylation of benzaldehyde catalyzed by (*S*)-**1**

Asymmetric allylations and propargylations of aromatic aldehydes are key C-C bond forming transformations, providing access to chiral homoallylic and homopropargyllic alcohols, respectively. It is well-established that, for these reactions, asymmetric induction can be

achieved by means of chiral organocatalysts.[13,14] Historically, both Lewis acids and bases have been used, but only the latter provide high degrees of setereoselectivity. Mechanistic studies of Kotora and coworkers[15-16] suggest that these reactions can proceed via two different mechanisms, depending on the solvent used. Under Nakajima's conditions,[8-10] using dichloromethane as solvent, it is generally accepted that the reaction follows the dissociative route shown in Figure 2.[17] In this case, the stereocontrolling step involves a chair-like transition state featuring a hexacoordinate silicon, in which both alkyl-aldehyde and aldehyde-silicon bonds are formed, as originally proposed by Denmark and coworkers.[18-22]

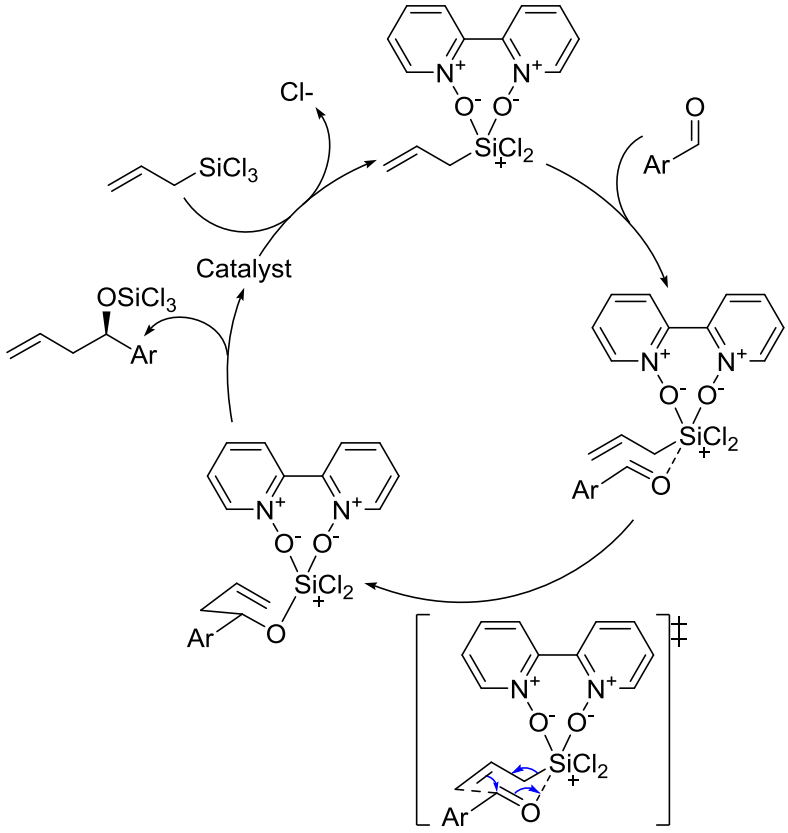


**Figure 2.** Catalytic cycle for the alkylation of aryl aldehydes catalyzed by a bipyridine N,N′-dioxide.

The well-organized coordination sphere around the silicon keeps the nucleophilic alkyl group, electrophile, and organocatalyst in close proximity, providing a chiral environment through a rigid, chair-like transition state that is not achievable when using a chiral Lewis acid as catalyst.[23] In the case of allylations catalyzed by (*S*)-**1**, Nakajima and co-workers[10] explained the

observed stereoselectivity based on the transition state model depicted in Figure 3a. This TS model was based in part on the observation that the stereoselectivity was independent of substitution at positions $R_1$ and $R_2$, but the *ee* was reduced to 49% in the presence of a methyl group at position $R_3$.[10] This latter observation was rationalized by steric interactions between this methyl group and the aromatic wall of the catalyst.

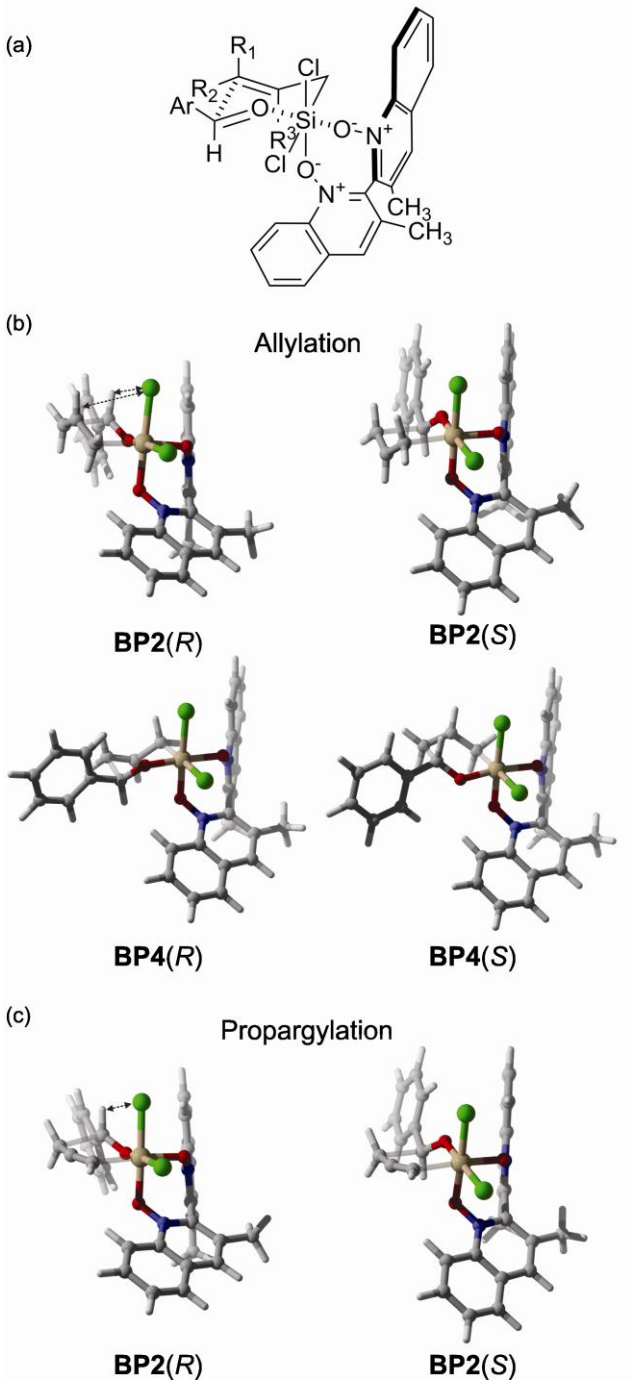

**Figure 3.** (a) Transition state model of Nakajima and co-workers[10] to explain the (*R*)-stereoselectivity of (*S*)-**1** in the allylation of aromatic aldehydes. Key TS structures for the (b) allylation and (c) propargylation of benzaldehyde. Stabilizing 1,3-diaxial interactions present in **BP2**(*R*) are indicated with dashed arrows.

Predicting the stereoselectivity of these reactions requires precise predictions of the relative free energy barriers for this stereocontrolling transition state. In particular, it is vital that the lowest-lying TS structures leading to the (*R*) and (*S*)-alcohols be predicted accurately. However, comparison of computationally predicted stereoselectivities with experimental *ee*'s alone is insufficient to gauge the accuracy of a given computational method (*vide infra*). Below, we assess the performance of popular DFT methods for allylation and propargylation reactions catalyzed by (*S*)-**1** while also explaining the origin of stereoselectivity in these reactions. The resulting TS model is qualitatively different from that proposed by Nakajima and co-workers,[10] but is consistent with our recent work on bipyridine *N*-oxide catalyzed alkylation reactions.[11-12] Together, these data provide key insights into the nature of bipyridine *N*,*N*′-dioxide catalyzed alkylation reactions, and pave the way for the rational design of more effective catalysts for both reactions.

## II. Computational Methods

Transition state geometries were optimized at six levels of theory, using different DFT functionals combined with commonly employed basis sets: B3LYP/6-31G(*d*),[24-25] B3LYP/TZV(2*d*,2*p*),[26] M06-2X/6-31+G(*d*,*p*),[27] B97-D/6-31G(*d*),[28-30] B97-D/TZV(2*d*,2*p*) and ω-B97X-D/TZV(2*d*,2*p*).[31] These geometry optimizations used the PCM model[32-33] to account for solvent effects (dichloromethane). Frequency calculations were performed at the same level of theory as the optimizations, and transition states were characterized by the existence of a single imaginary vibrational frequency. *ee*'s were predicted based on relative solution-phase free energies for all ten possible TS structures (*vide infra*), as done previously for bipyridine *N*-oxide catalyzed alkylations.[11-12] Free energies (T = 195K) were evaluated based on partition functions derived from the rigid-rotor and harmonic oscillator approximations.

Because DFT methods cannot be systematically improved, it is often necessary to benchmark results from DFT against more reliable, *ab initio* data. Often, this is done using CCSD(T) or related methods. However, such rigorous methods cannot be applied to systems of

the size considered here. Instead, for benchmarking purposes, gas-phase single point energies were evaluated at the B97-D/TZV(2*d*,2*p*) optimized TS geometries at the df-MP2/cc-pVTZ and LPNO-CEPA/1/def2-TZVP levels of theory.[34-38] The former method employs density fitting techniques to provide second-order Moller-Plesset perturbation theory (MP2) energies at greatly reduced computational costs, but with minimal loss in accuracy. The latter method, LPNO-CEPA/1, is an extension of the coupled-electron pair approximation (CEPA) based on local pair natural orbitals, and provides energies that are intermediate in quality between CCSD and CCSD(T).[35-36] However, unlike CCSD(T), LPNO-CEPA can be applied to relatively large molecules. Both of these ab initio methods were paired with large, triple-ζ quality basis sets. Gas-phase single point energies with the ωB97X-D,[31] M06-2X,[27] B2PLYP,[39-40] B2PLYP-D,[39-40] M05-2X,[41] and B3LYP[24-25] DFT functionals paired with commonly employed basis sets [6-31G(*d*), 6-31+G(*d*,*p*), and TZV(2*d*,2*p*)] were also computed at the B97-D/TZV(2*d*,2*p*) optimized geometries. All DFT computations were done using Gaussian09,[42] while Molpro[43] was used to compute df-MP2 energies and Orca 2.9.1[44] was used for the LPNO-CEPA computations.

## III. Results and Discussion

It is often assumed in the literature that, for bipyridine *N*-oxide and *N*,*N*′-dioxide catalyzed alkylation reactions, there is a single preferred ligand arrangement in which the chlorines adopt a *trans* arrangement and the alkyl nucleophile is located *trans* to an *N*-oxide (configuration **BP1** in Figure 4).[45-46] However, Lu, Wheeler, and co-workers[11-12] showed that, in the case of bipyridine *N*-oxides, there are ten feasible arrangements of ligands, giving rise to twenty possible TS structures [ten leading to the (*R*)-alcohol, ten leading to the (*S*)-alcohol]. Moreover, depending on the catalyst, any of these ligand configurations can be low-lying.[11-12] Consequently, for bipyridine *N*-oxide catalyzed alkylation reactions, one must consider all of these possible pathways in computations.

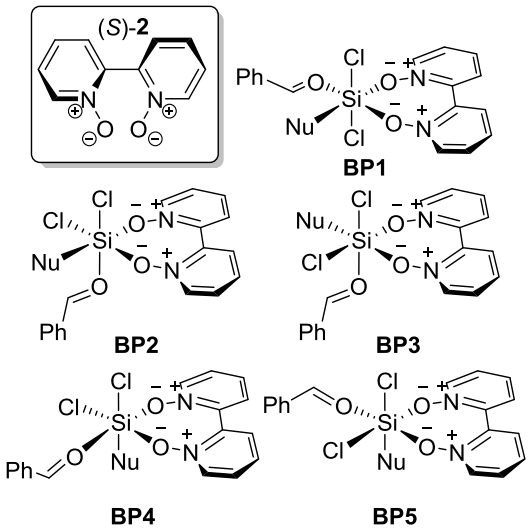


**Figure 4.** The five unique ligand configurations that are compatible with the alkylations of aromatic aldehydes catalyzed by $C_2$-symmetric bipyridine *N*,*N*′-dioxides. For each of the ligand configurations **BPX** (X = 1-5), there will be a pair of TS structures leading to the (*R*) and (*S*) alcohol, denoted **BPX**(*R*) and **BPX**(*S*), respectively. "Nu" refers to the alkyl nucleophile, which will be either an allyl group or allenyl group for allylations and propargylations, respectively.

The same will hold for bipyridine *N*,*N*′-dioxides catalyzed alkylations. In particular, for $C_2$-symmetric bipyridine *N*,*N*′-dioxide catalysts there are five possible arrangements of the alkyl nucleophile, aldehyde, and two chlorines around the hexacoordinate silicon that are compatible with the addition of the alkyl group to the aldehyde (**BP1**-**BP5** in Figure 4). For each of these configurations, the alkyl group can add to the *Si* or *Re* face of the aldehyde, leading to formation of the (*S*)- or (*R*)-alcohol, respectively. Thus, for a given $C_2$-symmetric catalyst, one must consider ten possible TS structures—five leading to formation of the (*R*) alcohol [**BP1**(*R*) – **BP5**(*R*)], and five leading to the (*S*) alcohol [**BP1**(*S*) – **BP5**(*S*)]. Nakajima's TS model (Figure 2)[10] corresponds to **BP4**(*R*).

All ten TS structures were located for both the allylation and propargylation of benzaldehyde catalyzed by (*S*)-**1** at six different levels of DFT theory. Key TS structures are shown in Figures 3b and 3c. The corresponding relative free energies are listed in Table 1, while the *ee*'s predicted from these relative free energies are listed in Table 2. Surprisingly, despite the structural similarities of the allylation and propargylation transition states, there was wide variation in predicted *ee*'s between these two reactions. In particular, the spread in predicted *ee*'s for the propargylation (0 to 99% *ee*) is significantly larger than that for the allylation (56 to

97% *ee*). Apparently, the stereoselectivity of the propargylation reaction is much more sensitive to theoretical method than the allylation.

A striking feature of the data presented in Table 1 is that, regardless of the level of theory, Nakajima's TS structure [**BP4**(*R*)] is significantly higher in free energy than the lowest-lying structure, **BP2**(*R*). Indeed, **BP4**(*R*) is among the least favorable TS structures, and will play no role in this reaction. This mirrors previous results for bipyridine *N*-oxide alkylations catalysts,[47-48] for which the originally-proposed TS models corresponded to relatively high-lying TS structures.[11-12] Additionally, the ligand configuration corresponding Nakajima's TS model leads to the opposite stereoselectivity compared to the experimental observation. That is, at all levels of theory considered, **BP4**(*R*) is higher in free energy than **BP4**(*S*), even though the TS model of Nakajima[10] was intended to explain the (*R*)-selectivity of (*S*)-**1**.

**Table 1.** Relative free energies (in kcal mol$^{-1}$) for the ten possible propargylation and propargylation transition states catalyzed by (*S*)-**1** using six levels of DFT theory, relative to the lowest-lying TS.

| | (*R*) Transition States | | | | | (*S*) Transition States | | | | |
|---|---|---|---|---|---|---|---|---|---|---|
| Method | **BP1** | **BP2** | **BP3** | **BP4** | **BP5** | **BP1** | **BP2** | **BP3** | **BP4** | **BP5** |
| | | | | | Allylation | | | | | |
| B97-D/TZV(2*d*,2*p*) | 4.0 | 0.0 | 8.2 | 7.0 | 5.5 | 3.1 | 1.1 | 2.1 | 4.9 | a |
| B97-D/6-31G(*d*) | 4.8 | 0.0 | 8.3 | 7.8 | 5.3 | 4.3 | 0.5 | 2.0 | 5.3 | a |
| ωB97X-D/TZV(2*d*,2*p*) | 4.0 | 0.0 | 8.7 | 5.0 | 5.3 | 3.1 | 1.1 | 2.0 | 4.3 | a |
| B3LYP/6-31G(*d*) | 2.5 | 0.0 | 8.4 | 6.7 | 4.7 | 2.0 | 1.8 | 2.6 | 3.5 | a |
| B3LYP/TZV(2*d*,2*p*) | 1.2 | 0.0 | 7.8 | 6.4 | 3.9 | 0.9 | 1.6 | 2.1 | 3.2 | a |
| M06-2X/6-31+G(*d*,*p*) | 5.7 | 0.0 | 9.5 | 9.6 | 6.1 | 3.1 | 1.6 | 2.8 | 5.6 | a |
| | | | | | Propargylation | | | | | |
| B97-D/TZV(2*d*,2*p*) | 3.2 | 0.0 | 6.2 | 6.1 | 3.6 | 3.3 | 0.8 | 1.2 | 4.9 | 7.5 |
| B97-D/6-31G(*d*) | 3.8 | 0.0 | 5.9 | 6.0 | 2.9 | 4.1 | 0.0 | 1.1 | 5.5 | 7.6 |
| ωB97X-D/TZV(2*d*,2*p*) | 4.1 | 0.0 | 7.7 | 8.1 | 4.6 | 4.9 | 2.0 | 2.7 | 6.5 | 9.5 |
| B3LYP/6-31G(*d*) | 0.8 | 0.0 | 5.6 | 5.2 | 2.8 | 1.7 | 0.3 | 1.1 | 3.4 | 7.1 |
| B3LYP/TZV(2*d*,2*p*) | 0.4 | 0.0 | 5.6 | 5.5 | 2.7 | 1.4 | 0.6 | 2.5 | 3.5 | 7.2 |
| M06-2X/6-31+G(*d*,*p*) | 2.9 | 0.0 | 7.2 | 7.7 | 3.8 | 3.8 | 1.0 | 0.7 | 5.9 | 9.2 |

[a]For the allylation, we were unable to locate TS structures corresponding to **BP5**(*S*) in which the (*S*)-**1** maintained both bonds to the silicon. The resulting pentacoordinate structures were 9 to 19 kcal mol$^{-1}$ higher in free energy than **BP2**(*R*).

A number of interesting observations can be made from the data in Table 2 regarding the performance of these DFT methods for these two reactions. First, we tested B97-D and B3LYP with two different basis sets, resulting in surprisingly different predicted *ee*'s. In particular,

although B97-D/TZV(2*d*,2*p*) provides stereoselectivities in general agreement with experiment for both the propargylation and allylation of benzaldehyde, when paired with the smaller 6-31G(*d*) basis set this functional predicts that **BP2**(*S*) is isoergonic with **BP2**(*R*). That is, B97-D/6-31G(*d*) predicts no stereoselectivity for the propargylation of benzaldehyde catalyzed by (*S*)-**1**. Although the B3LYP functional is somewhat less sensitive to basis set, the predicted *ee* for the propargylation reaction still changes by 40% going from the 6-31G(*d*) to the larger TZV(2*d*,2*p*) basis set. Satisfyingly, all of the methods but one, ωB97X-D/TZV(2*d*,2*p*), correctly predict that the propargylation reaction will be less stereoselective than the allylation; ωB97X-D/TZV(2*d*,2*p*) drastically overestimates the *ee* of the propargylation reaction. Moreover, other than B97-D/6-31G(*d*), all of the methods provide at least qualitatively corrected *ee*'s for both reactions, compared to experiment.

Unfortunately, despite the overall good performance of these methods in the prediction of experimental *ee*'s for these reactions (Table 2), the underlying relative free energies for the ten possible transition states are drastically different (see Table 1). In particular, there is no general agreement among these methods as to the identity of the lowest-lying TS leading to the (*S*)-alcohol. For example, for the allylation reaction, B3LYP/TZV(2*d*,2*p*) predicts that **BP1**(*S*) will be the lowest-lying TS structure leading to the (*S*)-alcohol, while the other levels of theory predict that **BP2**(*S*) will be lowest-lying. Similarly, while most of the other methods predict that **BP1**(*R*) will be at least 2.5 kcal mol$^{-1}$ higher in free energy than **BP2**(*R*), B3LYP/TZV(2*d*,2*p*) predicts **BP1**(*R*) to be only 1.2 kcal mol$^{-1}$ above **BP2**(*R*). These differences are important in understanding the stereoselectivity of these reactions, which will depend on the identity of the lowest-lying (*R*) and (*S*) transition states.

**Table 2.** Predicted *ee*'s for the allylation and propargylation of benzaldehyde catalyzed by (*S*)-**1** at six levels of theory, along with the experimental values.

| Method | Propargylation | Allylation |
|---|---|---|
| Experimental[8,10] | 52 | 88 |
| B97-D/TZV(2*d*,2*p*) | 73 | 88 |
| B97-D/6-31G(*d*) | 0 | 56 |
| ωB97X-D/TZV(2*d*,2*p*) | 99 | 87 |
| B3LYP/6-31G(*d*) | 33 | 97 |
| B3LYP/TZV(2*d*,2*p*) | 73 | 81 |
| M06-2X/6-31+G(*d*,*p*) | 61 | 96 |

Differences among predicted free energies for the low-lying TS structures are even more drastic for the propargylation reaction. For example, both B3LYP/6-31G(*d*) and B3LYP/TZV(2d,2p) predict that **BP1**(*R*) is relatively low-lying, compared to **BP2**(*R*), whereas the other methods predict **BP1**(*R*) to be at least 2.9 kcal $mol^{-1}$ higher in free energy than **BP2**(*R*). Similarly, M06-2X/6-31+G(*d*,*p*) predicts that **BP3**(*S*) is the favored TS leading to the (*S*)-alcohol. Again, these differences will qualitatively impact our understanding of the origin of stereoselectivity for this reaction. Unfortunately, there is no way to gauge the ability of these functionals to identify the low-lying TS structures for these reactions solely based on the overall *ee*'s.

## A. Computational Benchmark

To shed some light on the true energetic ordering of these possible TS structures, we compared gas-phase electronic energies computed using a range of DFT functionals with reliable *ab initio* benchmarks. This will allow us to identify DFT methods that correctly identify the lowest-lying (*R*) and (*S*) transition state structures and therefore provide physically-correct insight into the origin of stereoselectivity of these reactions. Gas-phase single-point energies were computed using ωB97X-D, M06-2X, M05-2X, B2PLYP-D, B2PLYP, B97-D, and B3LYP paired with three basis sets: 6-31G(*d*), 6-31+G(*d*,*p*) and TZV(2*d*,2*p*). All of these single point energies were evaluated at the B97-D/TZV(2*d*,2*p*) optimized geometries. The consideration of gas-phase energies allows us to compare against high-level LPNO-CEPA/1 results and assess the variation in underlying electronic energies predicted by these DFT methods in the absence of entropy and free energy corrections.

LPNO-CEPA/1 energies for the allylation transition states, relative to **BP2**(*R*), are listed in ESI Table S1, along with the *errors* in the relative energies from MP2 and seven different DFT functionals paired with three different basis sets. Analogous data for the propargylation reaction are shown in Table S2. The DFT predicted relative energies show a troubling degree of variation, with many predictions in error by nearly 5 kcal $mol^{-1}$ compared to the LPNO-CEPA/1 benchmark. Interestingly, these DFT functionals underestimate the energy of nearly all of the other TS structures relative to **BP2**(*R*). Moreover, the mean errors for all of these functionals increase with increasing basis set size. More importantly, B3LYP and B2PLYP predict **BP1**(*R*)

to lie lower in energy than **BP2**(*R*) for both reactions! However, LPNO-CPEA/1 predicts that **BP1**(*R*) lies 2.9 and 2.8 kcal $mol^{-1}$ higher in energy than **BP2**(*R*) for the allylation and propargylation reactions, respectively. Thus, from this data it appears that B3LYP is providing the correct *ee* for the propargylation reaction despite qualitatively incorrect underlying TS energies. On average, ωB97X-D and M06-2X provide TS electronic energies in closest agreement with the LPNO-CEPA/1 benchmark values.

In light of the good performance ωB97X-D/TZV(2*d*,2*p*) in predicting relative gas phase energies for the ten TS structures for the propargylation of benzaldehyde, it is rather surprising that ωB97X-D/TZV(2*d*,2*p*) overestimates the *ee* for the propargylation reaction (see Table 2). Apparently, for this reaction, the inclusion of entropic contributions and solvation free energies spoils the accuracy of ωB97X-D for the underlying electronic energies. B97-D/TZV(2*d*,2*p*), on the other hand, does a mediocre job predicting relative energies of these TS structures, with mean errors of -2.3 and -2.4 kcal $mol^{-1}$ for the allylation and propargylation reactions, respectively. However, this level of theory does provides reasonably good relative energies of the lowest-lying TS structures, which contributes to its ability to provide reliable predictions of the *ee*'s. Finally, even though B3LYP also provides sound predictions for **BP2**(*S*) relative to **BP2**(*R*), the overstabilization of **BP1**(*R*) by this functional prevents it from identifying the correct low-lying TS structures for these reactions. Overall, for our purposes, B97-D/TZV(2*d*,2*p*) appears to offer the best compromise between accuracy for key transition states and sound predictions of overall stereoselectivities, and will be used in future work to predict stereoselectivities of bipyridine *N*,*N*′-dioxide catalyzed alkylation reactions.

## B. Origin of Stereoselectivity in Alkylations Catalyzed by (*S*)-1

Having established that B97-D/TZV(2*d*,2*p*) correctly predicts both the overall stereoselectivity of bipyridine *N*,*N*′-dioxide catalyzed alkylation reactions (compared to experiment) and the relative energies of the key low-lying transition states (compared to computational benchmarks), we use this level of theory to unravel the origin of stereoselectivity in allylations and propargylations catalyzed by (*S*)-**1**. Nakajima *et al*.[10] explained the stereoselectivity of (*S*)-**1** based on the TS model depicted in Figure 3a. However, as noted above, the ligand configuration corresponding to this TS model is not only much higher in free energy

than other ligand configurations, but predicts the wrong stereoselectivity. Instead, the stereoselectivity of (*S*)-**1** for the allylation of benzaldehyde arises from the 1.1 kcal $mol^{-1}$ difference in free energy between **BP2**(*R*) and **BP2**(*S*) (see Figure 3b). This free energy difference can be explained by favorable 1,3-diaxial interactions between two C–H bonds and one of the chlorines in **BP2**(*R*), which are absent in **BP2**(*S*). Indeed, for all five (*R*, *S*) pairs of TS structures, the lower lying structure is the one in which these two C–H bonds are aligned with one of the Si–Cl bonds. This was observed previously for bipyridine *N*-oxide catalyzed allylations,[12] and appears to be a general, but largely unrecognized, source of enantiodifferentiation in this family of reactions. Qualitatively, these stabilizing interactions can be understood in terms of favorable alignment of the local dipoles of the C–H and Si–Cl bonds, and this model is similar in spirit to previous explanations of the *E*/*Z* selectivity in the addition of allylboronates to aldehydes from Hoffmann and Landmann.[49]

The reduced stereoselectivity in the case of the propargylation catalyzed by (*S*)-**1**, compared to the allylation, stems from the smaller free energy difference between **BP2**(*R*) and **BP2**(*S*) for this reaction. That this free energy difference is smaller than the corresponding difference for the allylation reaction simply reflects the lack of a central C–H bond in the allenyl group. That is, in the allylation reaction there are two C–H bonds that can engage in favorable 1,3-diaxial interactions with the Cl, whereas there is only one in the propargylation reaction (see Figures 3b and 3c).

Finally, we note that Nakajima's TS model (Figure 3a)[10] was based in part on the observation that methyl substitution at position $R_3$ lead to reduced *ee*'s. This was attributed to steric interactions between this methyl group and the catalyst. Instead, the reduced selectivity in this case stems from the removal of the central C–H bond in the allyl group. Indeed, the selectivity for the allylation reaction in which $R_3$ = Me (49% *ee*)[10] is commensurate with the 52% *ee* reported for the propargylation by (*S*)-**1**. In both cases, the reduced stereoselectivity arises from a lack of a C–H bond at this central position on the alkyl group.

### C. Inherent Stereoselectivities of Bipyridine *N*,*N*′-Dioxides

Following previous work by Lu, Wheeler, and co-workers,[11-12] we next turn to (*S*)-bipyridine *N*,*N*′-dioxide, (*S*)-**2**, as a model catalyst in order to gain more general insight into the

stereoselectivity of bipyridine *N*,*N*′-dioxides in asymmetric alkylations (see Figure 4). This simple model catalyst enables the study of the inherent stereoselectivity of the five possible ligand arrangements in the absence of other catalyst components. Table 5 shows the predicted relative free energies barriers for the ten possible TS structures for the allylation and propargylation of benzaldehyde catalyzed by (*S*)-**2**, along with the difference between the (*R*, *S*) pairs of TS structures for a given ligand configuration (**BPX**)

First, for this model system, **BP2**(*R*) is low-lying for both the allylation and propargylation reaction, as was observed for (*S*)-**1**. Furthermore, **BP2**(*S*) is 1.1 and 0.4 kcal mol$^{-1}$ higher in free energy than **BP2**(*R*) for the allylation and propargylation, respectively, which is also consistent with the data for (*S*)-**1**. Interestingly, the present data predict that the model catalyst (*S*)-**2** will provide stereoselectivities equal to that for Nakajima's catalyst (*S*)-**1** for the allylation of benzaldehyde! This provides further evidence that the stereoselectivity of (*S*)-**1** for allylation reactions stems primarily from the electrostatic interactions with the chiral electrostatic environment of the hexacoordinate silicon, and not other interactions between the catalyst and substrate. Overall, the general agreement between the relative free energies for catalyst (*S*)-**1** and model catalyst (*S*)-**2** suggests that the latter can serve as a proxy for more complex bipyridine *N*,*N*′-dioxide catalysts. The extent to which the computed data for (*S*)-**2** can be generalized to a broader range of bipyridine *N*,*N*′-dioxide based catalysts will be addressed in future work.[50]

**Table 5**. B97-D/TZV(2*d*,2*p*) predicted relative free energy barriers for the formation of the R and S alcohol for (*S*)-**2** catalyst, along with the difference in the free energies for the (*R*) and (*S*) pathway for each ligand configuration (**BPX**), all in kcal mol$^{-1}$.

| | Allylation | | | Propargylation | | |
|---|---|---|---|---|---|---|
| | *R* | *S* | Diff. | *R* | *S* | Diff. |
| **BP1** | 2.1 | 2.0 | 0.1 | 1.2 | 1.2 | 0.0 |
| **BP2** | 0.0 | 1.1 | -1.1 | 0.0 | 0.4 | -0.4 |
| **BP3** | 6.6 | 2.2 | 4.4 | 5.8 | 1.7 | 4.1 |
| **BP4** | 5.6 | 4.1 | 1.5 | 4.5 | 4.1 | 0.4 |
| **BP5** | 5.0 | 8.4 | -3.4 | 2.8 | 3.5 | -0.7 |

For the allylation reaction catalyzed by (*S*)-**2**, **BP2**(*S*) is the only transition state within 2 kcal mol$^{-1}$ of **BP2**(*R*). This suggests that, unlike for bipyridine *N*-oxide catalyzed alkylations,[24,25] it might be safe to consider only this ligand configuration when predicting stereoselectivities for bipyridine *N*,*N*′-dioxide catalyzed allylations.[51] However, for the analogous propargylation

reaction, the possible TS structures are slightly more closely packed energetically, with four transition states falling within 2 kcal $mol^{-1}$ of **BP2**(*R*). As such, it will be necessary to consider at least several of the possible ligand configurations when predicting stereoselectivities of bipyridine *N*,*N*′-dioxide catalyzed propargylations.

More to the point, we see that for allylations catalyzed by bipyridine *N*,*N*′-dioxides, all but one of the ligand configurations (**BP1**) leads to significant differences in free energy between the (*R*) and (*S*) transition states, even in the absence of other chiral components of the catalyst. That is, many of these ligand configurations lead to significant differentiation between the (*R*) and (*S*) barrier heights merely through the impact of the chiral environment of the hexacoordinate silicon. This was observed previously for bipyridine *N*-oxide catalyzed alkylations by Lu, Wheeler, and co-workers.[11] Consistent with the results for (*S*)-**1**, we once again find that the lower-lying TS structure for a given ligand arrangement always features a geometry with the aldehyde and allyl C–H bonds aligned with one of the Si-Cl bonds, whereas the TS structures with these C–H bonds directed away from the Si–Cl bond are always higher in free energy. The lack of a significant free energy difference between **BP1**(*R*) and **BP1**(*S*) can be explained by the *trans* arrangement of the chlorines, because, in this case, the C–H bonds are aligned with Si–Cl bonds in both **BP1**(*R*) and **BP1**(*S*).

For the propargylation reactions, this inherent stereoselectivity is much smaller than for the allylation—for a given ligand arrangement, the free energy gap between the (*R*) and (*S*) structures is less for the propargylation reaction than for the allylation reaction. That is, propargylation reactions are inherently less stereoselective than allylations. Again, this mirrors previous results for bipyridine *N*-oxides from Lu, Porterfield, and Wheeler,[12] and reflects the lack of a central C–H bond in the allenyl group. Indeed, for the propargylation reaction, only a single ligand configuration (**BP3**) is inherently highly stereoselective. This suggest that highly stereoselective catalysts for the propargylation of benzaldehyde can be built on a bipyridine *N*,*N*′-dioxide scaffold by devising a catalyst that steers the reaction towards ligand arrangement **BP3**, while blocking access to the other, less stereoselective ligand arrangements. Alternatively, a stereoselective bipyridine *N*,*N*′-dioxide propargylation catalyst can be designed by introducing elements that preferentially stabilize **BP2**(*R*) over **BP2**(*S*). Both strategies for propargylation catalyst design are currently being pursued.

## IV. Summary and Conclusions

We assessed the performance of several popular DFT functionals for the prediction of stereoselectivities for the allylation and propargylation of benzaldehyde catalyzed by Nakajima's bipyridine *N*,*N*′-dioxide, (*S*)-**1**.[10] Satisfyingly, most of these functionals predict *ee*'s in qualitative agreement with experiment. Unfortunately, this agreement with experiment appears to be fortuitous in some cases, since some of these functionals predict the incorrect low-lying TS structures. These data should serve as warnings that the reproduction of experimental *ee*'s alone is insufficient to guarantee that a given theoretical method is predicting the correct stereocontrolling transition state structures. Moreover, several methods tested performed significantly better for allylations than propargylations, despite the outward similarity of these two reactions. The reliable predictions of stereoselectivities by a given DFT approach for one reaction does not guarantee its performance for even very similar transformations. Overall, of the DFT methods tested here, B97-D/TZV(2*d*,2*p*) seems to provide the best compromise of accuracy for individual TS structures and predictions of stereoselectivites.

We also provided a new explanation for stereoselectivity in allylations and propargylations catalyzed by (*S*)-**1**. Ultimately, we showed that favorable 1,3-diaxial interactions between C–H bonds on the aldehyde and allyl group and one of the chlorines underlie the stereoselectivity in allylation reactions. The reduced stereoselectivity in the case of bipyridine *N*,*N*′-dioxide catalyzed propargylations arises from the lack of a central C–H bond in the allenyl group. Unfortunately, Nakajima's transition state model (Figure 3a)[10] is based on the incorrect arrangement of ligands surrounding the hexacoordinate silicon and actually leads to preferential formation of the (*S*)-alcohol, in contrast with the experimental observations. This is because the ligand configuration in Nakajima's TS model (**BP4**) is inherently selective for formation of the (*S*)-alcohol (see Table 5).

Unlike bipyridine *N*-oxide catalyzed allylation reactions, for *N*,*N*′-dioxide catalyzed allylations we found that a single transition state **BP2**(*R*) is favored over the others and is likely operative in all bipyridine *N*,*N*′-dioxide catalyzed allylations. On the other hand, for bipyridine *N*,*N*′-dioxide catalyzed propargylation reactions, several different ligand configurations could come into play in these reactions, as was seen for bipyridine *N*-oxide catalyzed reactions.[11-12] Ultimately, the present results point towards two possible strategies for the rational design of

bipyridine *N*,*N*′-dioxide catalysts for asymmetric propargylations. In particular, highly stereoselective catalysts can be designed by devising catalysts that steer the reaction towards the highly inherently stereoselective ligand arrangement **BP3**, or that preferentially stabilize **BP2**(*R*) over **BP2**(*S*). These strategies are currently being pursued, and will be discussed in further detail in a forthcoming publication.

## ACKNOWLEDGMENT

This work was supported by The Welch Foundation (Grant A-1775) and the National Science Foundation (Grant CHE-1266022). We also thank the Texas A&M Supercomputing Facility for providing computational resources.

## REFERENCES

(1) Houk, K. N.; Cheong, P. H.-Y. *Nature* **2008**, *455*, 309-313.
(2) Cheong, P. H.-Y.; Legault, C. Y.; Um, J. M.; Çelebi-Olçüm, N.; Houk, K. N. *Chem. Rev.* **2011**, *111*, 5042–5137.
(3) Sunoj, R. B. *WIREs Comp. Mol. Sci.* **2011**, *1*, 920-931.
(4) Lu, T.; Porterfield, M. A.; Wheeler, S. E. *Org. Lett.* **2012**, *14*, 5310-5313.
(5) Lu, T.; Zhu, R.; An, Y.; Wheeler, S. E. *J. Am. Chem. Soc.* **2012**, *134*, 3095-3102.
(6) Lu, T.; Wheeler, S. E. *Chem. Eur. J.* **2013**, *19*, 15141-15147.
(7) Lu, T.; Wheeler, S. E. *Org. Lett.* **2014**, *16*, 3268-3271.
(8) Nakajima, M.; Saito, M.; Hashimoto, S. *Tetrahedron-Asymmetr* **2002**, *13*, 2449-2452.
(9) Nakajima, M.; Saito, M.; Hashimoto, S. *Chem Pharm Bull* **2000**, *48*, 306-307.
(10) Nakajima, M.; Saito, M.; Shiro, M.; Hashimoto, S. *J Am Chem Soc* **1998**, *120*, 6419-6420.
(11) Lu, T. X.; Zhu, R. X.; An, Y.; Wheeler, S. E. *J Am Chem Soc* **2012**, *134*, 3095-3102.
(12) Lu, T.; Porterfield, M. A.; Wheeler, S. E. *Org Lett* **2012**.
(13) Haruta, R.; Ishiguro, M.; Ikeda, N.; Yamamoto, H. *J Am Chem Soc* **1982**, *104*, 7667-7669.
(14) Ikeda, N.; Arai, I.; Yamamoto, H. *J Am Chem Soc* **1986**, *108*, 483-486.
(15) Malkov, A. V.; Ramirez-Lopez, P.; Biedermannova, L.; Rulisek, L.; Dufková, L.; Kotora, M.; Zhu, F.; Kočovky, P. *J. Am. Chem. Soc.* **2008**, *130*, 5341-5348.
(16) Hrdina, R.; Opekar, F.; Roithová, J.; Kotora, M. *Chem. Commun.* **2009**, 2314-2316.
(17) Hrdina, R.; Opekar, F.; Roithova, J.; Kotora, M. *Chem Commun* **2009**, 2314-2316.
(18) Denmark, S. E.; Coe, D. M.; Pratt, N. E.; Griedel, B. D. *J Org Chem* **1994**, *59*, 6161-6163.
(19) Denmark, S. E.; Fu, J. P. *J. Am. Chem. Soc.* **2000**, *122*, 12021-12022.
(20) Denmark, S. E.; Wynn, T. *J. Am. Chem. Soc.* **2001**, *123*, 6199-6200.
(21) Denmark, S. E.; Fu, J. P. *J. Am. Chem. Soc.* **2001**, *123*, 9488-9489.
(22) Denmark, S. E.; Beutner, G. L. *Angewandte Chemie-International Edition* **2008**, *47*, 1560-1638.
(23) Denmark, S. E.; Fu, J. P. *Chem Commun* **2003**, 167-170.
(24) Becke, A. D. *Journal of Chemical Physics* **1993**, *98*, 1372-1377.

(25) Lee, C. T.; Yang, W. T.; Parr, R. G. *Phys Rev B* **1988**, *37*, 785-789.
(26) Schafer, A.; Huber, C.; Ahlrichs, R. *J. Chem. Phys.* **1994**, *100*, 5829-5835.
(27) Zhao, Y.; Truhlar, D. G. *Theor Chem Acc* **2008**, *120*, 215-241.
(28) Becke, A. *J. Chem. Phys.* **1997**, *107*, 8554-8560.
(29) Grimme, S. *J Comput Chem* **2006**, *27*, 1787-1799.
(30) Grimme, S. *Wires Comput Mol Sci* **2011**, *1*, 211-228.
(31) Chai, J.-D.; Head-Gordon, M. *J. Chem. Phys.* **2008**, *128*, 084106.
(32) Tomasi, J.; Mennucci, B.; Cammi, R. *Chem Rev* **2005**, *105*, 2999-3093.
(33) Miertus, S.; Scrocco, E.; Tomasi, J. *Chem. Phys.* **1981**, *55*, 117-129.
(34) Dunning, T. H., Jr. *J. Chem. Phys.* **1989**, *90*, 1007-1023.
(35) Neese, F.; Wennmohs, F.; Hansen, A. *J. Chem. Phys.* **2009**, *130*, 114108.
(36) Neese, F.; Wennmohs, F.; Hansen, A.; Grimme, S. *Acc. Chem. Res.* **2009**, *42*, 641-648.
(37) Kollmar, C.; Neese, F. *Mol. Phys.* **2010**, *108*, 2449-2458.
(38) Weigend, F.; Ahlrichs, R. *Phys. Chem. Chem. Phys.* **2005**, *7*, 3297-3305.
(39) Grimme, S. *J. Chem. Phys.* **2006**, *124*, 034108.
(40) Schwabe, T.; Grimme, S. *Phys. Chem. Chem. Phys.* **2007**, *9*, 3397-3406.
(41) Zhao, Y.; Schultz, N. E.; Truhlar, D. G. *J. Chem. Theory and Comput.* **2006**, *2*, 364-382.
(42) *Gaussian 09, Revision B.01, Frisch, M. J., et al. Gaussian, Inc., Wallingford CT, 2009.*
(43) *MOLPRO, version 2010.1, is a package of ab initio programs written by H.-J. Werner, et al.*
(44) Neese, F. *WIREs Comp. Mol. Sci.* **2012**, *2*, 73-78.
(45) Musher, J. I. *Angew. Chem. Chem. Int. Ed. Engl.* **1969**, *8*, 54-68.
(46) Tandura, S. N.; Voronkov, M. G.; Alekseev, N. V. *Top. Curr. Chem.* **1986**, *131*, 99-189.
(47) Takenaka, N.; Chen, J. S.; Captain, B. *Org. Lett.* **2011**, *13*, 1654-1657.
(48) Malkov, A. V.; Orsini, M.; Pernazza, D.; Muir, K. W.; Langer, V.; Meghani, P.; Kočovsky, P. *Org. Lett.* **2002**, *4*, 1047-1049.
(49) Hoffmann, R. W.; Landmann, B. *Chem. Ber.* **1986**, *119*, 1039-1053.
(50) Rooks, B. J.; Haas, M. R.; Sepúlveda, D.; Lu, T.; Wheeler, S. E. *ACS Catalysis* **submitted**.
(51) Of course, for some catalysts there could be significant steric (or other) interactions that render a different ligand configuration low-lying.

Graphical Abstract

# Performance of DFT Methods and Origin of Stereoselectivity in Bipyridine *N,N′*-Dioxide Catalyzed Allylation and Propargylation Reactions

Diana Sepúlveda-Camarena, Tongxiang Lu, and Steven E. Wheeler*

*Department of Chemistry, Texas A&M University, College Station, TX 77843*

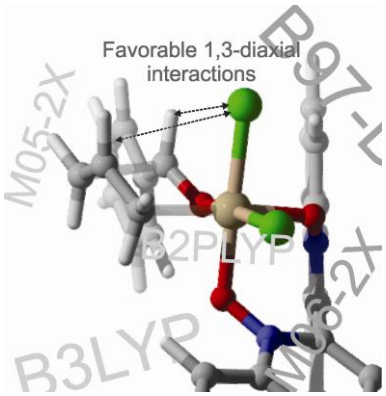


It is shown that many DFT methods correctly predict the stereoselectivity of bipyridine N,N'-dioxide catalyzed alkylation reactions despite predicting the incorrect low-lying transition state structures. A novel explanation of the origin of stereoselectivity in these reactions is also provided.